

## Sliding Mode Speed Controller for a Vector Controlled Double Star Induction Motor

**Abstract.** This paper presents a speed sliding mode controller for a vector controlled (FOC) double star induction motor (DSIM) fed by a two pulse width modulation voltage source inverters. The machine has two sets of three-phase windings which are spatially phase shifted by 30 electrical degrees with isolated neutrals. The sliding mode control (SMC) is used to achieve robust performance against parameter variations and external disturbances. The problem with this conventional controller is that it has large chattering on the torque and the drive is very noisy. In order to reduce a torque ripple, the sign function is used. The proposed algorithm was simulated by Matlab/Simulink software and simulation results show that the performance of the control scheme is robust and the chattering problem is solved.

**Streszczenie.** Zaprezentowano sterownik ślizgowy silnika indukcyjnego DSIM zasilanego z przekształtnika dwu-pulsowego z modulacją napięcia. Sterownik taki zastosowano dla uzyskania odporności na zewnętrzne zakłócenia. (Sterownik ślizgowy do silnika indukcyjnego typu DSIM)

**Keywords:** DSIM, FOC, and SMC.

**Słowa kluczowe:** in the case of foreign Authors in this line the Editor inserts Polish translation of keywords.

### Introduction

The field-oriented control technique has been widely used in industry for high-performance induction machine (IM) drive, where the knowledge of synchronous angular velocity is often necessary in the phase transformation for achieving the favorable decoupling control. However, the control performance of the IM is still influenced by the variations of motor parameters, especially the rotor time-constant, which varies with the temperature and the saturation of the magnetizing inductance, the uncertainties, such as mechanical parameter variation, external disturbance, unstructured uncertainty due to non ideal field orientation in transient state, and unmodelled dynamics, etc.. [1, 2, 3]. The Double Star Induction Motor (DSIM) has two sets of three-phase windings which are spatially phase shifted by 30 electrical degrees with isolated neutrals. Therefore, modeling and control of this machine in the original reference frame would be very difficult. For this reason, some assumptions must be made in order to obtain a simplified model Park to control it. The sinusoidal voltage waveforms are generated by a two voltage source inverters (VSI) and the control method presented is indirect rotor field oriented control (IFOC) with stator currents regulation [5, 6, 7, 8, 9]. The motivation of this study is to design a suitable control scheme to confront the uncertainties existed in practical applications of an indirect field-oriented DSIM drive. One of the possible approaches to the robust control of the uncertain systems has been found in variable structure systems and sliding mode control [3,4,10,11].

The sliding mode controller has been suggested to achieve robust performance against parameter variations and load disturbances. It also offers a fast dynamic response, stable control system and easy hardware-software implementation. On the other hand, this control method offers some drawbacks associated with the large torque chattering that appears in steady state. Chattering involves high-frequency control switching and may lead to excitation of unmodelled high frequency system dynamics. Chattering also causes high heat losses in electronic systems and undue wear in mechanical systems [3]. In order to reduce the system chattering a sign function is used.

In this paper, by means of the advantage of SMC a synthetic control scheme is presented. The sliding mode controller (SMC) is designed for the speed regulation of an indirect vector controlled DSIM fed by a two voltage source inverters. The simulation results show that our method can achieve very robust and satisfactory performance.

### DSIM mathematic model

The study presented in this paper is based on the following assumptions: The air gap is uniform and the windings are sinusoidally distributed around the air gap. The magnetic saturation and core losses are neglected.

The DSIM has two sets of three-phase windings spatially shifted by 30 electrical degrees with isolated neutral points. Fig.1 shows the representation of the DSIM

The Park model in set of equation of state is presented below [6-7].

Voltage equations:

$$(1) \quad \begin{cases} [V_{abc,s1}] = [R_{s1}][I_{abc,s1}] + \left[ \frac{d\phi_{abc,s1}}{dt} \right] \\ [V_{abc,s2}] = [R_{s2}][I_{abc,s2}] + \left[ \frac{d\phi_{abc,s2}}{dt} \right] \\ [0] = [R_r][I_{abc,r}] + \left[ \frac{d\phi_{abc,r}}{dt} \right] \end{cases}$$

Flux equations

$$(2) \quad \begin{cases} \left[ \begin{matrix} \phi_{abc,s1} \\ \phi_{abc,s2} \\ \phi_{abc,r} \end{matrix} \right] = \begin{bmatrix} [L_{s1,s1}] & [L_{s1,s2}] & [L_{s1,r}] \\ [L_{s2,s1}] & [L_{s2,s2}] & [L_{s2,r}] \\ [L_{r,s1}] & [L_{r,s2}] & [L_{r,r}] \end{bmatrix} \left[ \begin{matrix} [I_{abc,s1}] \\ [I_{abc,s2}] \\ [I_{abc,r}] \end{matrix} \right] \end{cases}$$

With:

$$\begin{aligned} [V_{abc,s1}] &= [v_{as1} \ v_{bs1} \ v_{cs1}]^T; \\ [V_{abc,s2}] &= [v_{as2} \ v_{bs2} \ v_{cs2}]^T; \\ [I_{abc,s1}] &= [i_{as1} \ i_{bs1} \ i_{cs1}]^T; [I_{abc,s2}] = [i_{as2} \ i_{bs2} \ i_{cs2}]^T \\ [V_{abc,r}] &= [0] = [v_{ar} \ v_{br} \ v_{cr}]^T; [I_{abc,r}] = [i_{ar} \ i_{br} \ i_{cr}]^T \\ [R_{s1}] &= [R_{s2}] = \text{diag}[R_s]_{3 \times 3}; [R_r] = \text{diag}[R_r]_{3 \times 3} \end{aligned}$$

Flux linkage

$$\begin{aligned} [L_{s1,s1}] &= \begin{bmatrix} l_{s1} + l_{ms} & -l_{ms}/2 & -l_{ms}/2 \\ -l_{ms}/2 & l_{s1} + l_{ms} & -l_{ms}/2 \\ -l_{ms}/2 & -l_{ms}/2 & l_{s1} + l_{ms} \end{bmatrix} \\ [L_{s2,s2}] &= \begin{bmatrix} l_{s2} + l_{ms} & -l_{ms}/2 & -l_{ms}/2 \\ -l_{ms}/2 & l_{s2} + l_{ms} & -l_{ms}/2 \\ -l_{ms}/2 & -l_{ms}/2 & l_{s2} + l_{ms} \end{bmatrix} \\ [L_{r,r}] &= \begin{bmatrix} l_r + l_{mr} & -l_{mr}/2 & -l_{mr}/2 \\ -l_{mr}/2 & l_r + l_{mr} & -l_{mr}/2 \\ -l_{mr}/2 & -l_{mr}/2 & l_r + l_{mr} \end{bmatrix} \end{aligned}$$

$$\begin{aligned}
& [L_{s1,s2}] \\
& = l_{ms} \begin{bmatrix} \cos(\alpha) & \cos(\alpha + 2\pi/3) & \cos(\alpha + 4\pi/3) \\ \cos(\alpha + 4\pi/3) & \cos(\alpha) & \cos(\alpha + 2\pi/3) \\ \cos(\alpha + 2\pi/3) & \cos(\alpha + 4\pi/3) & \cos(\alpha) \end{bmatrix} \\
& [L_{s1,r}] \\
& = l_{sr} \begin{bmatrix} \cos(\theta_s) & \cos(\theta_s + 2\pi/3) & \cos(\theta_s + 4\pi/3) \\ \cos(\theta_s + 4\pi/3) & \cos(\theta_s) & \cos(\theta_s + 2\pi/3) \\ \cos(\theta_s + 2\pi/3) & \cos(\theta_s + 4\pi/3) & \cos(\theta_s) \end{bmatrix} \\
& [L_{s2,r}] = l_{sr} \begin{bmatrix} \cos(\gamma) & \cos(\gamma + 2\pi/3) & \cos(\gamma + 4\pi/3) \\ \cos(\gamma + 4\pi/3) & \cos(\gamma) & \cos(\gamma + 2\pi/3) \\ \cos(\gamma + 2\pi/3) & \cos(\gamma + 4\pi/3) & \cos(\gamma) \end{bmatrix}
\end{aligned}$$

with :

$$\gamma = \theta_s - \alpha; [L_{s2,s1}] = [L_{s1,s2}]^T;$$

$$[L_{r,s1}] = [L_{s1,r}]^T; [L_{r,s2}] = [L_{s2,r}]^T$$

$R_s, l_{s1} = l_{s2}$  and  $l_{ms}$  are the stator resistance, the leakage stator inductance and the magnetizing stator inductance respectively.

$R_r, l_r$ , and  $l_{mr}$  are the rotor resistance, the leakage rotor inductance and the magnetizing rotor inductance respectively.

The electromagnetic torque can be expressed as follows [6-7]:

$$(3) \quad T_e = [I_{abc,s1}] \frac{d}{d\theta} [L_{s1,r}] [I_{abs,r}] + [I_{abc,s2}] \frac{d}{d\theta} [L_{s2,r}] [I_{abs,r}]$$

In the reference frame at the rotating field 'd q', the electrical DSIM Park model and the rotor speed are presented below [5].

$$(4) \quad \left\{ \begin{aligned} \frac{d\phi_{ds1}}{dt} &= V_{ds1} - \frac{R_s}{l_{s1}} (\phi_{ds1} - \phi_{dm}) + \omega_s \phi_{qs1} \\ \frac{d\phi_{qs1}}{dt} &= V_{qs1} - \frac{R_s}{l_{s1}} (\phi_{qs1} - \phi_{qm}) - \omega_s \phi_{ds1} \\ \frac{d\phi_{ds2}}{dt} &= V_{ds2} - \frac{R_s}{l_{s2}} (\phi_{ds2} - \phi_{dm}) + \omega_s \phi_{qs2} \\ \frac{d\phi_{qs2}}{dt} &= V_{qs2} - \frac{R_s}{l_{s2}} (\phi_{qs2} - \phi_{qm}) - \omega_s \phi_{ds2} \\ \frac{d\phi_{dr}}{dt} &= V_{dr} - \frac{R_r}{l_r} (\phi_{dr} - \phi_{dm}) + (\omega_s - \omega_r) \phi_{qr} \\ \frac{d\phi_{qr}}{dt} &= V_{qr} - \frac{R_r}{l_r} (\phi_{qr} - \phi_{dm}) - (\omega_s - \omega_r) \phi_{dr} \\ J \frac{d\Omega}{dt} &= T_e - T_L - K_f \Omega \\ C_e &= p \frac{l_m}{l_m + l_r} [\phi_{dr} (I_{qs1} + I_{qs2}) - \phi_{qr} (I_{ds1} + I_{ds2})] \end{aligned} \right.$$

With:

$$(5) \quad \left\{ \begin{aligned} \phi_{dm} &= l_m (I_{ds1} + I_{ds2} + I_{dr}) \\ \phi_{qm} &= l_m (I_{qs1} + I_{qs2} + I_{qr}) \\ \phi_{ds1} &= l_{s1} I_{ds1} + \phi_{dm} \\ \phi_{qs1} &= l_{s1} I_{qs1} + \phi_{qm} \\ \phi_{ds2} &= l_{s2} I_{ds2} + \phi_{dm} \\ \phi_{qs2} &= l_{s2} I_{qs2} + \phi_{qm} \\ \phi_{dr} &= l_r I_{dr} + \phi_{dm} \\ \phi_{qr} &= l_r I_{qr} + \phi_{qm} \end{aligned} \right. \\ \phi_s &= \sqrt{(\phi_{ds1} + \phi_{ds2})^2 + (\phi_{qs1} + \phi_{qs2})^2}$$

The terms used in the previous expressions are the following:

$V_{ds1}, V_{qs1}, V_{ds2}, V_{qs2}$ : Respectively stator voltages in 'd' axis and 'q' axis of 1 and 2

$I_{ds1}, I_{qs1}, I_{ds2}, I_{qs2}$ : Respectively stator currents in 'd' axis and 'q' axis of 1 and 2

$I_{dr}, I_{qr}$  rotor currents in 'd' axis and 'q' axis

$\phi_{ds1}, \phi_{qs1}, \phi_{ds2}, \phi_{qs2}$ : Respectively stator fluxes in 'd' axis and 'q' axis of 1 and 2

$\omega_r, \omega_s$ : Rotor speed and natural frequency;  $p$ : Pole number of the rotor;  $T_e$ : Electromagnetic torque

$T_L$ : Load torque;  $J$ : Inertia system

$K_f$ : Friction coefficient; In the induction machines, rotor windings are short circuited hence, i.e.  $V_{dr} = V_{qr} = 0$ .

### VSI Modeling

PWM is used in power electronics to "digitalize" the power so that a sequence of voltage pulses can be generated by the on and off for the power converter. Then, the PWM-VSI is expressed by the imposed sequencings at semiconductors which realize modulation of voltages applied to stator windings. Voltages at load neutral point, for one SVI, can be given by the following expression:

$$(6) \quad \begin{bmatrix} v_a \\ v_b \\ v_c \end{bmatrix} \frac{V_d}{6} \begin{bmatrix} 2 & -1 & -1 \\ -1 & 2 & -1 \\ -1 & -1 & 2 \end{bmatrix} \begin{bmatrix} S_1 \\ S_2 \\ S_3 \end{bmatrix}$$

$S_i$  ( $i = 1,2,3$ ): Logic signal  $V_d$ : direct voltage

### DSIM Field oriented control

The application of the field oriented control consists on the orientation of the rotor flux vector along the 'd' axis [6-7] which can be expressed by considering  $\phi_{dr} = \phi_r^*$  and  $\phi_{qr} = 0$ . Consequently, the dynamic equations (3) after arrangement yield to:

- The relationship between torque and flux:

$$(7) \quad T_e^* = p \frac{l_m}{l_m + l_r} (I_{qs1} + I_{qs2}) \phi_r^*$$

- The relation between slip speed and stator currents

$$(8) \quad \omega_{sl}^* = \frac{R_r}{l_m + l_r} (I_{qs1} + I_{qs2})$$

- The relations between voltages and currents components are:

$$(9) \quad \begin{cases} V_{ds1}^* = R_s I_{ds1} + s l_{s1} I_{ds1} - \omega_s^* (l_{s1} I_{qs1} + T_r \phi_r^* \omega_{sl}^*) \\ V_{qs1}^* = R_s I_{qs1} + s l_{s1} I_{qs1} + \omega_s^* (l_{s1} I_{ds1} + \phi_r^*) \\ V_{ds2}^* = R_s I_{ds2} + s l_{s2} I_{ds2} - \omega_s^* (l_{s2} I_{qs2} + T_r \phi_r^* \omega_{sl}^*) \\ V_{qs2}^* = R_s I_{qs2} + s l_{s2} I_{qs2} + \omega_s^* (l_{s2} I_{ds2} + \phi_r^*) \end{cases}$$

where,  $T_r = \frac{l_r}{R_r}$  is time rotor constant.

The voltage expressions show that the axes 'd q' are not independents, so, for a decoupling system, it is necessary to introduce new variables.

$$(10) \quad \begin{cases} V_{ds1-c} = \omega_s^* (l_{s1} I_{qs1} + T_r \phi_r^* \omega_{sl}^*) \\ V_{qs1-c} = \omega_s^* (l_{s1} I_{ds1} + \phi_r^*) \\ V_{ds2-c} = \omega_s^* (l_{s2} I_{qs2} + T_r \phi_r^* \omega_{sl}^*) \\ V_{qs2-c} = \omega_s^* (l_{s2} I_{ds2} + \phi_r^*) \end{cases}$$

and

$$(11) \quad \begin{cases} V_{ds1} = R_s I_{ds1} + s l_{s1} I_{ds1} \\ V_{qs1} = R_s I_{qs1} + s l_{s1} I_{qs1} \\ V_{ds2} = R_s I_{ds2} + s l_{s2} I_{ds2} \\ V_{qs2} = R_s I_{qs2} + s l_{s2} I_{qs2} \end{cases}$$

The equation system (11) shows that stator voltages are directly related to stator currents. To compensate the error introduced at decoupling time, the voltage references at constant flux are given by

$$(12) \quad \begin{cases} V_{ds1}^* = V_{ds1} - V_{ds1_c} \\ V_{qs1}^* = V_{qs1} - V_{qs1_c} \\ V_{ds2}^* = V_{ds2} - V_{ds2_c} \\ V_{qs2}^* = V_{qs2} - V_{qs2_c} \end{cases}$$

For a perfect decoupling, we add stator currents regulation loops  $I_{ds1}, I_{qs1}, I_{ds2}, I_{qs2}$  and we obtain at their output stator voltages  $V_{ds1}, V_{qs1}, V_{ds2}, V_{qs2}$ . The regulation goal is to assure a good performance for internal current loops. In this work, indirect field oriented control (IFOC) with PWM source voltage inverter which fed the DSIM is studied. So, the SMCs and FSMCs have been tested for the IFOC decoupling block and the speed controller. The flux is generally maintained constant at its nominal value through the field weakening block described by a nonlinear function. According to the above analysis, the DSIM block diagram with speed controller and IFOC strategy is shown in fig. 2.

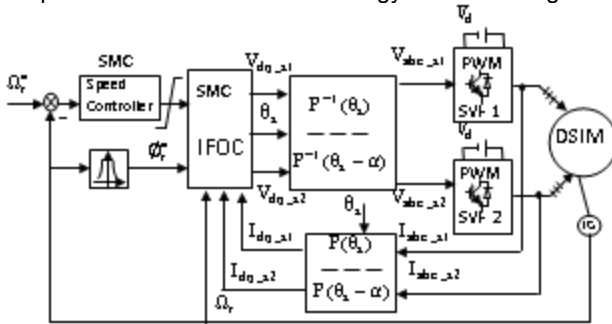


Fig.1. IFOC scheme for DSIM

### Sliding mode control design

The basic principle of the sliding mode control consists in moving the state trajectory of the system toward a surface  $S(X) = 0$  and maintaining it around this surface with the switching logic function  $U_n$ . The basic sliding mode control law is expressed as.

$$(13) \quad U_c = U_{eq} + U_n$$

This expression uses two terms,  $U_{eq}$  and  $U_n$ .  $U_{eq}$  is determined off line with a model that represents the plant as accurately as possible. It is used when the system state is in the sliding mode. The term  $U_n$  is a sign function defined as  $U_n = k \operatorname{sgn}(S(X))$ , where

$$(14) \quad \operatorname{sgn}(S(X)) = \begin{cases} 1 & \text{if } S(X) < 0 \\ -1 & \text{if } S(X) > 0 \end{cases}$$

This will guarantee that the state is attracted to the switching surface by satisfying the Lyapunov stability criteria shown in (15)

$$(15) \quad S(X) \dot{S}(X) < 0$$

This strategy enforces the system trajectory to move toward and to stay on the sliding surface from any initial condition. Using a sign function often causes chattering in practice. One solution to reduce chattering is to introduce a boundary layer around the sliding surface [5],[6]. This is expressed by

$$(16) \quad U_n = \begin{cases} \frac{k}{\varepsilon} S(X) & \text{if } |S(X)| < \varepsilon \\ k \operatorname{sgn}(S(X)) & \text{if } |S(X)| > \varepsilon \end{cases}$$

with  $k$ , a positive coefficient and  $\varepsilon$ , the thickness of the boundary layer. However, a small value of  $\varepsilon$  might produce a boundary layer so thin that it can excite high frequency dynamics [7].

### DSIM Sliding Mode Control

The proposed control scheme is a cascade structure as it is shown in Fig. 2, in which five surfaces are required. The 'd' axis, has two stator current component ( $I_{ds1}, I_{ds2}$ ) loops and the 'q' axis, the internal loops allow the control stator current components ( $I_{qs1}, I_{qs2}$ ), whereas the external loop provide the regulation of the speed.

### Speed SMC

Under field oriented assumptions, the electromagnetic torque can be expressed as:

$$(17) \quad T_e = \frac{p l_m}{l_m + l_r} (I_{qs1} + I_{qs2}) \phi_r^* = k_T I_{qs}$$

where,  $k_T$  is the torque constant and  $\phi_r^*$  is the flux reference.

To design a sliding mode speed controller for the double star induction motor FOC drive, consider the mechanical equation:

$$(18) \quad \frac{J}{p} \dot{\Omega}_r + \frac{K_f}{p} \Omega_r + T_L = T_e$$

where  $\Omega_r$  is the rotor speed in electrical rad/s, rearranging to get

$$(19) \quad \dot{\Omega}_r = \frac{p}{J} T_e - \frac{K_f}{J} \Omega_r - \frac{p}{J} T_L$$

Considering  $\Delta a$  and  $\Delta b$  as bounded uncertainties introduced by system parameters  $J$  and  $K_f$ , (19) can be rewritten as:

$$(20) \quad \dot{\Omega}_r = (a + \Delta a) \Omega_r + (b + \Delta b) T_e + c T_L$$

where  $a = -\frac{K_f}{J}$ ,  $b = \frac{p}{J}$ ,  $c = -\frac{p}{J}$

Defining the state variable of the speed error as:

$$(21) \quad e(t) = \Omega_r(t) - \Omega_r^*(t)$$

Combining (14) with (15) and taking the derivative of (15) yields

$$(22) \quad \dot{e}(t) = ae(t) + b\{\bar{T}_e + d(t)\}$$

where  $d(t)$  is the lumped uncertainty defined as:

$$(23) \quad d(t) = \frac{\Delta a}{b}\Omega_r(t) + \frac{\Delta b}{b}T_e + \frac{c}{b}T_L$$

And

$$(24) \quad \bar{T}_e(t) = T_e(t) + \frac{a}{b}\Omega^*$$

Defining a switching surface  $s(t)$  from the nominal values of system parameters  $a$  and  $b$  [7-9]:

$$(25) \quad s(t) = e(t) - \int_0^t (a + bk)e(\tau) d\tau$$

Such that the error dynamics at the sliding surface  $s(t) = \dot{s}(t) = 0$  will be forced to exponentially decay to zero, then the error dynamics can be described by:

$$(26) \quad \dot{e}(t) = (a + bk)e(t)$$

where  $k$  is a linear negative feedback gain [9]. The variable structure speed controller law can be defined as:

$$(27) \quad \bar{T}_e = ke(t) - \beta \text{sign}(s(t))$$

where  $\beta$  is known as hitting control gain used to make the sliding mode condition possible and the sign function can be defined as [9]:

$$(28) \quad \text{sign}(s) = \begin{cases} 1 & \text{if } s > 0 \\ 0 & \text{if } s = 0 \\ -1 & \text{if } s < 0 \end{cases}$$

The final electromagnetic torque command  $T_e^*$  of the output of the sliding mode speed controller can be obtained by directly substituting (27) into (24). Basically, the control law for  $T_e^*$  is divided into two parts: equivalent control  $U_{eq}$  which defines the control action when the system is on the sliding mode and switching part  $U_s$  which ensures the existence condition of the sliding mode. If the friction  $k_f$  is neglected expressions for  $U_{eq}$  and  $U_s$  can be written as:

$$(29) \quad \begin{cases} U_{eq} = ke(t) \\ U_s = -\beta \text{sign}(s(t)) \end{cases}$$

To guarantee the existence of the switching surface consider a Lyapunov function [6-9]:

$$(30) \quad V(t) = \frac{1}{2}s^2(t)$$

Based on Lyapunov theory, if the function  $\dot{V}(t)$  is negative definite, this will ensure that the system trajectory will be driven and attracted toward the sliding surface  $s(t)$  and once reached, it will remain sliding on it until the origin is reached asymptotically [6]. Taking the derivative of (30) and substituting from the derivative of (25):

$$(31) \quad \dot{V}(t) = s(t)\dot{s}(t) = s(t)\{\dot{e}(t) - (a + bk)e(t)\} \leq 0$$

Substitute from (19) into (28):

$$(32) \quad s(t)\dot{s}(t) = s(t)\{b\bar{T}_e(t) + bd(t) - bke(t)\}$$

Using (27) gives

$$(33) \quad s(t)\dot{s} = s(t)\{-\beta \text{sign}(s(t)) - d(t)\} \leq 0$$

To ensure that (32) will be always negative definite, the value of the hitting control gain  $\beta$  should be designed as the upper bound of the lumped uncertainties  $d(t)$ , i.e.

$$(34) \quad \beta \geq |d(t)|$$

However, it is difficult practically to estimate the bound of uncertainties in (23). Therefore the hitting control gain  $\beta$  has to be chosen large enough to overcome the effect of any external disturbance [5], [6]. Therefore the speed control law defined in (27) will guarantee the existence of the switching surface  $s(t)$  in (25) and when the error function  $e(t)$  reaches the sliding surface, the system dynamics will be governed by (26) which is always stable [10]. Moreover, the control system will be insensitive to the uncertainties  $\Delta a$ ,  $\Delta b$  and the load disturbance  $T_L$ .

### Current SMCs

In this work four current sliding mode surfaces are defined as follows:

$$(35) \quad \begin{cases} S(I_{qs1}) = I_{qs1}^* - I_{qs1} \\ S(I_{qs2}) = I_{qs2}^* - I_{qs2} \\ S(I_{ds1}) = I_{ds1}^* - I_{ds1} \\ S(I_{ds2}) = I_{ds2}^* - I_{ds2} \end{cases}$$

The control law development for each variable in sliding mode theory is deduced from the reaching condition (15) and is indicated below

The current regulators laws in the 'd' axis and 'q' axis can be written as:

*Current sliding mode control law of  $I_{qs1}$*

$$(36) \quad S(I_{qs1}) \cdot \dot{S}(I_{qs1}) < 0 \Rightarrow V_{qs1}^s = V_{qs1\_eq} + V_{qs1\_n}$$

$$(37) \quad V_{qs1\_eq} = R_s I_{qs1} + l_{s1} I_{qs1} + \omega_s^* (l_{s1} I_{ds1} + \Phi_r^*)$$

$$V_{qs1\_n} = \begin{cases} \frac{k_{q1}}{\varepsilon_{q1}} S(I_{qs1}) & \text{if } |S(I_{qs1})| < \varepsilon_{q1} \\ k_{q1} \text{sgn}(S(I_{qs1})) & \text{if } |S(I_{qs1})| > \varepsilon_{q1} \end{cases}$$

*Current sliding mode control law of  $I_{qs2}$*

$$(39) \quad S(I_{qs2}) \cdot \dot{S}(I_{qs2}) < 0 \Rightarrow V_{qs2}^s = V_{qs2\_eq} + V_{qs2\_n}$$

$$(40) \quad V_{qs2\_eq} = R_s I_{qs2} + l_{s2} I_{qs2} + \omega_s^* (l_{s2} I_{ds2} + \Phi_r^*)$$

$$(41) \quad V_{qs2\_n} = \begin{cases} \frac{k_{q2}}{\varepsilon_{q2}} S(I_{qs2}) & \text{if } |S(I_{qs2})| < \varepsilon_{q2} \\ k_{q2} \text{sgn}(S(I_{qs2})) & \text{if } |S(I_{qs2})| > \varepsilon_{q2} \end{cases}$$

*Current sliding mode control law of  $I_{ds1}$*

$$(42) \quad S(I_{ds1}) \cdot \dot{S}(I_{ds1}) < 0 \Rightarrow V_{ds1}^s = V_{ds1\_eq} + V_{ds1\_n}$$

$$(43) \quad V_{ds1\_eq} = R_s I_{ds1} + l_{s2} I_{ds1} + \omega_s^* (l_{s2} I_{qs1} + T_r \Phi_r^* \omega_{sl}^*)$$

$$(44) \quad V_{ds1\_n} = \begin{cases} \frac{k_{d1}}{\varepsilon_{d1}} S(I_{ds1}) & \text{if } |S(I_{ds1})| < \varepsilon_{d1} \\ k_{d1} \text{sgn}(S(I_{ds1})) & \text{if } |S(I_{ds1})| > \varepsilon_{d1} \end{cases}$$

*Current sliding mode control law of  $I_{ds2}$*

$$(45) \quad S(I_{ds2}) \cdot \dot{S}(I_{ds2}) < 0 \Rightarrow V_{ds2}^s = V_{ds2\_eq} + V_{ds2\_n}$$

$$(46) \quad V_{ds2\_eq} = R_s I_{ds2} + l_{s2} I_{ds2} + \omega_s^* (l_{s2} I_{ds2} + T_r \Phi_r^* \omega_{sl}^*)$$

$$(47) \quad V_{ds2\_n} = \begin{cases} \frac{k_{d2}}{\varepsilon_{d2}} S(I_{ds2}) & \text{if } |S(I_{ds2})| < \varepsilon_{d2} \\ k_{d2} \text{sgn}(S(I_{ds2})) & \text{if } |S(I_{ds2})| > \varepsilon_{d2} \end{cases}$$

To verify the system stability condition, the gains  $k_{d1}$ ,  $k_{d2}$ ,  $k_{q1}$ ,  $k_{q2}$  and  $\varepsilon_{d1}$ ,  $\varepsilon_{d2}$ ,  $\varepsilon_{q1}$ ,  $\varepsilon_{q2}$  should be taken positive by selecting the appropriate values.

### Simulation results and discussions

The proposed scheme has been implemented with Matlab/Simulink in order to evaluate its performance. The DSIM used for the simulations has the following parameters:

$P = 4,5\text{kw}$ ,  $U_n = 220/380\text{ V}$ ,  $f = 50\text{Hz}$ ,  $I_n = 6.5\text{A}$   
 $R_{s1} = R_{s2} = 3.72\Omega$ ,  $R_r = 2.12\Omega$   
 $L_{s1} = L_{s2} = 0.022\text{H}$ ,  $L_r = 0.006\text{H}$ ,  $L_m = 0.3672\text{H}$   
 $J = 0.0625\text{kg. m}^2$ ,  $p = 2$ ,  $k_f = 0.001\text{Nm. s/rad}$

First we present the simulated results of the IFOC system for DSM where command input is step reference for speed with load torque variation. The speed regulator

and the IFOC decoupling block are controlled by SMCs. It can be seen that the speed response present better tracking characteristics. The external disturbance (load torque) on the speed response is rejected instantaneously. Better decoupled properties are obtained and fluxes track the desired fluxes precisely.

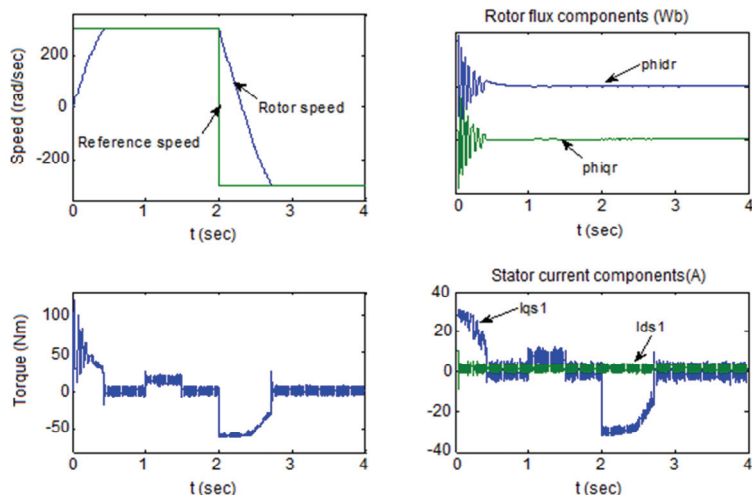


Fig.2 Speed, torque, flux and stator current responses with rotor speed inversed command and load variations

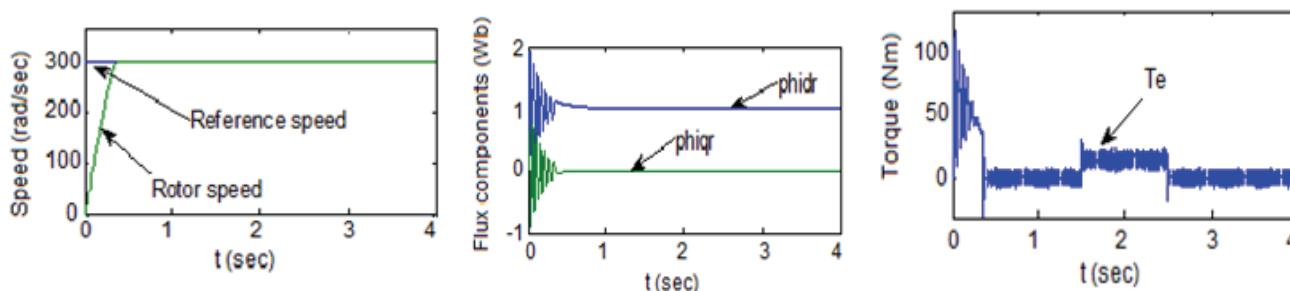


Fig.3 Speed, torque and flux responses with SMC

## Conclusion

The results obtained show the applicability of this control technique in the field of the electric drives. The objective of continuation is very good. The speed time response and the perturbation rejection are very good with no overshoot.

Decoupling is maintained even with the inversion of the speed.

The SMCs have very interesting dynamic performances and provide a stable system with satisfactory performances with a good decoupling.

## REFERENCES

- [1] V. I. Utkin, "Variable structure systems with sliding modes", Transactions on Automatic Control, 22(1977), pp. 212-221.
- [2] V.I. Utkin B., "sliding mode control design principles and applications to electric drives", IEEE, Trans on IE, 40(1999).
- [3] A. Meroufel, A. Massoum, and P. Wira "A Fuzzy Sliding Mode Controller for a Vector Controlled Induction Motor", Industrial Electronics, 2008. ISIE 2008. IEEE International Symposium on Publication, pp. 1873-1878(2008),
- [4] C.Y.Won, D.H.Kim, S.C.Kim and D.W.Yoo " New fuzzy sliding mode controller for position control of induction motor". IEEE, Proc. Of APEC'93, pp 115-121(1993)
- [5] E. Merabet, R. Abdessmed, H. Amimeur and F. Hamoudi, "Field oriented control of a dual star induction machine using fuzzy regulators," in 4th Int. Conf. Computer

Integrated Manufacturing, CIP'07, Univ. Setif, Algeria, Nov. 03–04, 2007.

- [6] Bojoi, A. Tenconi, G. Griva and F. Profumo, "Vector control of dual three-phase induction-motor drives two current sensors," RIEEE Trans. Ind. Appl., vol. 42, no. 5, pp. 1284–1292, Sep./Oct. 2006
- [7] R. Bojoi, M. Lazzari, F. Profumo and A. Tenconi, "Digital Field-Oriented Control for Dual Three-Phase Induction Motor Drives", IEEE Trans. On INDUSTRY Appl., Vol. 39, No. 3, May/June 2003, pp. 752-760
- [8] G. K. Singh, K. Nam and S. K. Lim, "A simple indirect field-oriented control scheme for multiphase induction machine," IEEE Trans Ind.Electron vol. 52, no. 4, pp. 1177–1184, Aug. 2005
- [9] A. Hazzab, I. K. Bousserhane and M. Kamli, "Design of a fuzzy sliding mode controller by genetic algorithms for induction machine speed control," Int. Journal Emerging Elec. Power Syst.,
- [10] Dragan Antic, Marko Milojkovic, Sasa Nikolic, "Fuzzy Sliding Mode Control with Additional Fuzzy Control Component" Facta Universitatis, Series: Automatic Control and Robotics Vol. 8, No 1, 2009, pp. 25 – 34

Ahmed MASSOUM, Abdelkader MEROUFEL, Abderrahim BENTAALLAH  
 University Djillali Liabes of Sidi Bel-Abbès, Algeria